18. Anderson, M. A., Gieselmann, M. J. & Xu, Q. *J. Membrane Sci.* **392,** 43 (1988).
19. O'Regan, B., Moser, J., Anderson, M. & Grätzel, M. *J. phys. Chem.* **94,** 8720–8726 (1990).

ACKNOWLEDGEMENTS. We are grateful to I. Rodicio for experimental help, to M. Nazzeruddin for a sample of sensitizer and to A. Kay for advice on the preparation of colloidal membranes. This work was supported by the Swiss National Energy Office.

Super-spiral structures in an excitable medium

V. Perez-Muñuzuri*, R. Aliev, B. Vasiev, V. Perez-Villar* & V. I. Krinsky

Institute of Theoretical and Experimental Biophysics, Academy of Sciences USSR, 142292 Pushchino, Moscow Region, USSR
* Departamento Fisica de la Materia Condensada, Facultad de Fisicas, E-15706 University of Santiago de Compostela, Spain

ROTATING spiral waves have been observed in various excitable media, including heart muscle[1], retinae[2], cultures of the slime mould *Dyctiostelium discoideum*[3,4] and chemical oscillators such as the Belousov–Zhabotinsky (BZ) reaction[5–7]. Under certain conditions the spiral wave does not exhibit simple periodic rotation, but quasiperiodic[8] (or 'compound'[9]) rotation, in which the spiral's origin (the tip) meanders[10]. Recent calculations[11] have shown that highly meandering tip motion can impose superstructures on spiral waves. Here we reproduce these patterns experimentally, using the BZ reaction as the excitable medium. We induce high tip meander by applying pulses of electrical current locally at the tip[12]. Image processing of the patterns reveals a spiral wave of larger wavelength superimposed on the original wave, an effect that can be described in terms of a Doppler shift in the original spiral.

All our experiments were performed in a BZ reaction[13] in silica gel at room temperature (20 °C). A 0.9-mm-thick gel layer containing ferroin (0.008 M) was prepared in a Petri dish. During the experiments this layer was covered with a thick (6–8 mm) solution of the other BZ reaction components: 0.1 M $NaBrO_3$, 0.1 M $CH_2(COOH)_2$ and 0.5 M H_2SO_4.

The highly meandering tip motion needed for the production of superstructures was enhanced by using stepwise pulses of electric current[12] with a period of 11 min. In each period, the voltage (1.5 V, ~5 mA) was switched on for 4 min.

The electrical circuit used (analogous to that in ref. 12) included two electrodes immersed in the liquid layer. One of these was a circular electrode which ran around the border of the Petri dish, the other was needle-shaped (0.6 mm diameter). The needle was placed over the spiral tip (3 mm into the liquid layer). Two different types of electrodes, stainless steel and platinum, were used, with the same results.

The spiral wave dynamics were followed with a video recorder connected to a PC computer. To observe super-spiral waves, simple image processing was carried out: after acquiring two successive images (separated by 2 min), we subtracted the second from the first. This same procedure was used in the calculations of ref. 11. Contrast enhancement was then used to improve the quality of the printed pictures.

Spiral waves with many turns were created by the following procedure: at the beginning of the experiment, the sulphuric acid concentration was reduced (to ~0.2 M) to avoid the spontaneous appearance of wave sources. Spiral waves were produced in this medium by the breaking of a circular wave. To increase the frequency and the number of spiral turns, sulphuric acid was added until it reached its final concentration (0.5 M). This procedure made it possible to create a single vortex of ~14 turns, with period $T_s \approx 94$ s and wavelength $\lambda_s \approx 0.34$ cm (Fig. 1).

After the medium had become homogeneous, the spiral waves were perturbed by switching the current on and off. This resulted in the successive increasing and diminishing of the size of the core[12], so that the spiral tip described a 'flowerlet' pattern. The ratio of two frequencies associated with this motion was about six.

When this highly meandering tip motion occurs, the spiral shape becomes asymmetric. Some of the wavefronts that make up the spiral approach each other (see Fig. 2*a*). When the picture is processed by subtracting one image from another, a superstructure appears with the shape of a spiral wave (Fig. 2*b*). This super-spiral does not disappear with time, but rotates as the base spiral does; the tips of both spirals always coincide (Fig. 3). Note that the same results were observed numerically[11] (compare upper and lower parts of Fig. 2).

The period and wavelength of the super-spiral ($T_{ss} \approx 540$ s and $\lambda_{ss} \approx 2$ cm) proved to be six times as great as those of the base spiral. In contrast, the linear velocity was roughly equal for both spirals.

The super-spiral can be considered to be the result of the approach between fronts of the base spiral. In this case, the wave period detected at any point in the medium changes periodically with time. Figure 4*a* shows this effect, measured at a point near the centre of Fig. 2*a*.

The results presented in Fig. 4*a* can be interpreted by the Doppler effect. If we suppose that the waves of the spiral are emitted by a source rotating around a circle at constant velocity v_1 and period T_{ss}, then the period of waves at any point in the medium is given by the equation

$$T(t) = T_s\left\{1 + \frac{v_1}{v_0}\cos\left(2\pi\frac{t}{T_{ss}} + \phi\right)\right\} \qquad (1)$$

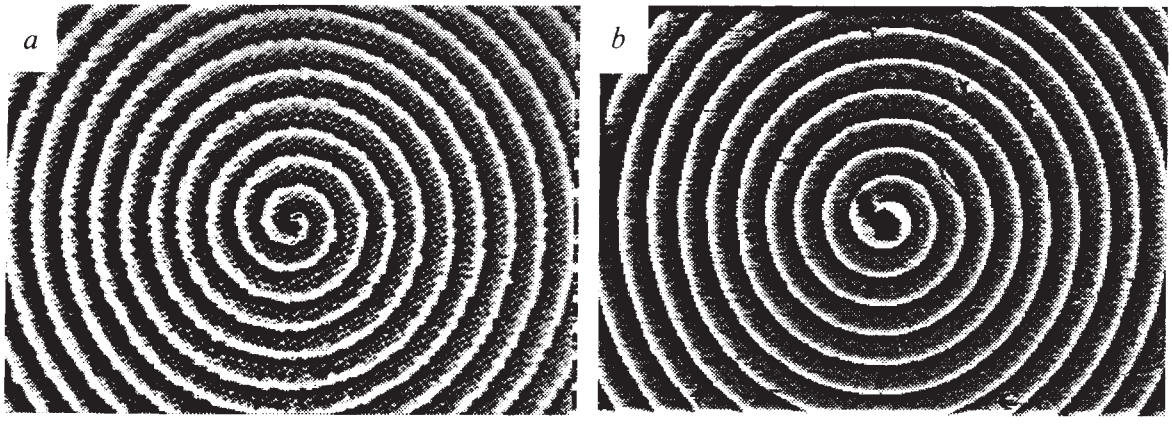

FIG. 1 Rigidly rotating spiral waves (*a*) for the phase-reaction/diffusion equation, $d\varphi/dt = R\{1 - \delta \sin(\varphi)\} + \alpha\nabla^2\varphi + \beta|\nabla\varphi|^2$ (refs 11 and 15; and P. Hanusse and V.P.M., manuscript in preparation) and (*b*) in the BZ reaction. The appearance and behaviour in the two cases are strikingly similar: constant wavelength, sharp fronts and rigid rotation around the centre. The black spot in the centre of *b* is the electrode shadow.

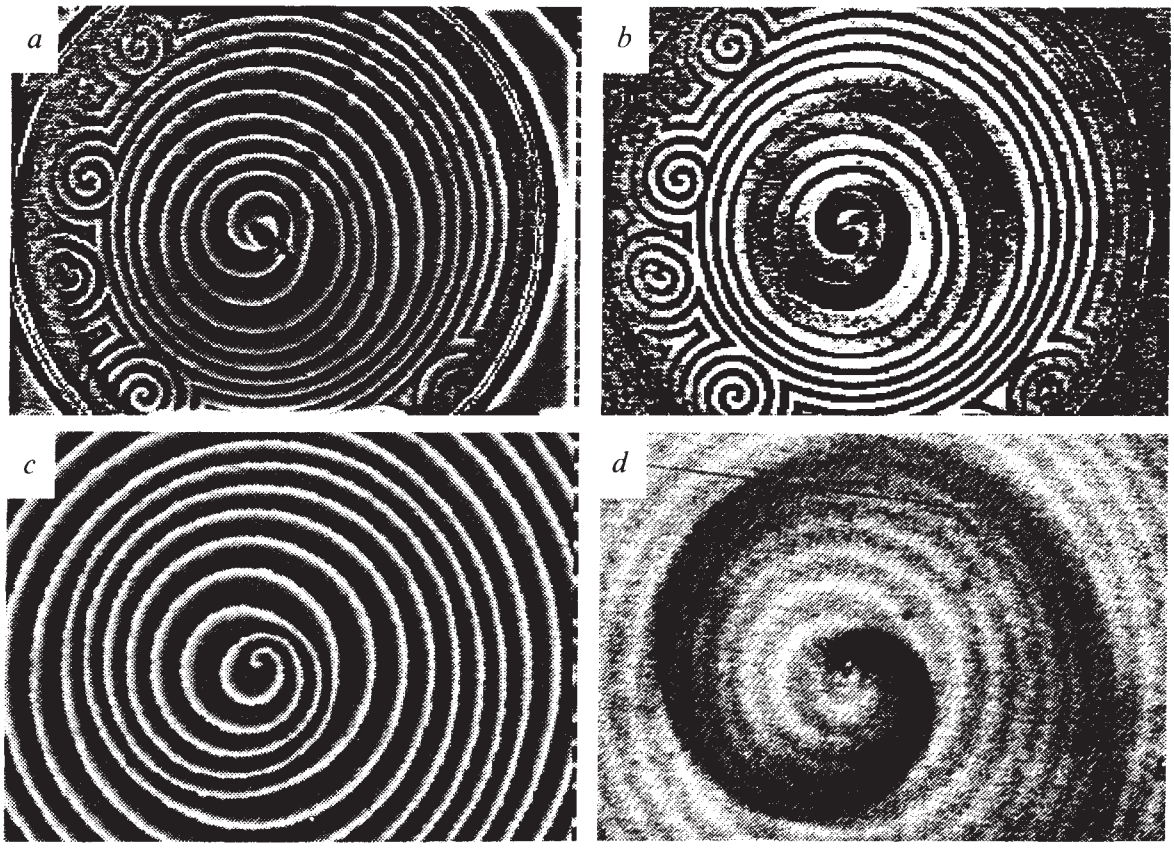

FIG. 2 Experimental and numerical highly meandering spiral and super-spiral waves. *a*, Stepwise electric current (the electrode shadow is seen in the upper part of the picture) was used to enhance the meandering tip motion. *c*, The model[11] predicts similar behaviour. Super-spiral waves (*b* and *d*) superimposed on the non-rigidly rotating vortices (*a* and *c*) can be observed after simple image processing has been carried out (see text). Note that the super-spiral wavelength is six times greater than that of the base spiral.

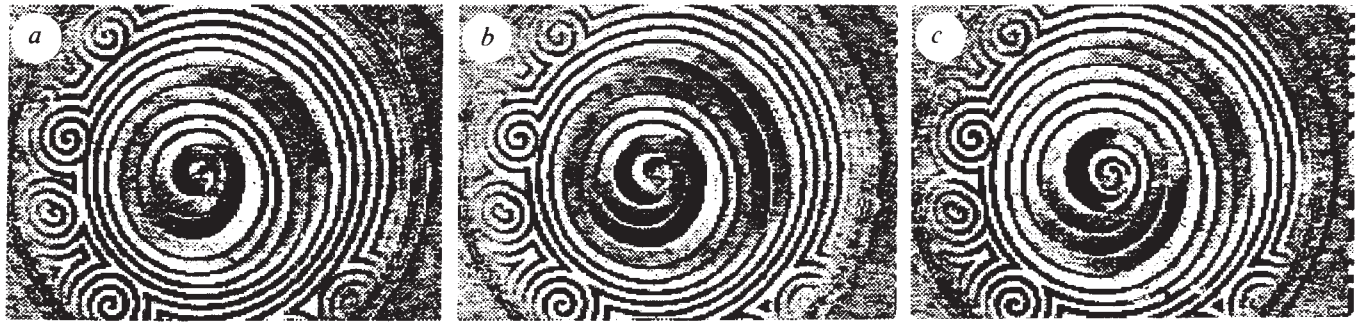

FIG. 3 The rotation of the super-spiral wave in the BZ reaction. The time interval between the frames was 160 s. Far from the core, the super-spiral becomes indistinct because of dispersion and diffusion processes.

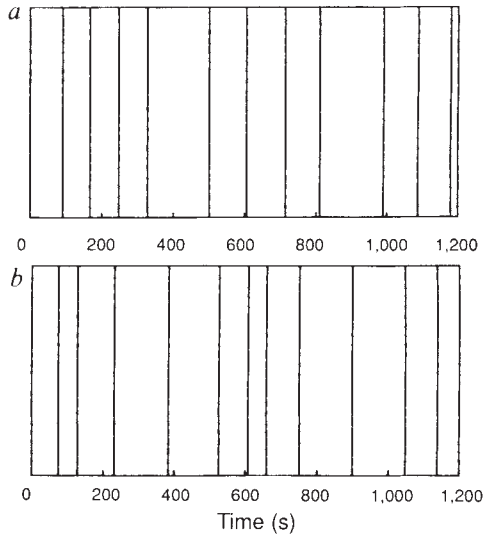

FIG. 4 Doppler effect in BZ reactions. Wavefront positions are represented by vertical lines for (*a*) a point near the spiral centre in Fig. 2*a*, and (*b*) in simulation. In equation (1), $v_1/v_0=0.5$ and $\phi=\pi/3$; other parameters do not affect the observed behaviour.

where v_0 and T_s are the velocity and period of the emitted waves, and ϕ is a phase shift.

Figure 4*b* shows the periodic behaviour of $T(t)$ when $t = nT_s$ ($n = 1, 2 \ldots$). These results are qualitatively similar to those shown in Fig. 4*a*. In both cases, two regions, with small and large intervals between waves, can be differentiated. The differences between the figures can be attributed to two processes occurring in the BZ reaction: first, the trajectory of the tip is more complicated than in our simulations; and second, diffusion and dispersion effects were not considered.

The effect on the super-spiral behaviour of the relative length of time for which the current is switched on and off has not been studied in detail; work is currently in progress (V.P.M. *et al.*, manuscript in preparation). By controlling this parameter, it is possible to decrease the wavelength of the super-spiral and observe the transition to spatiotemporal irregular motion, as was described in ref. 11.

Note that electric current was used only to enhance the meandering; its use is not strictly necessary for super-spirals to occur. Such structures can be observed in the BZ reaction even without external stimulation, although in this case the vortices show weak meandering. For such vortices, dispersion and diffusion processes occurring in the BZ reaction result in the waves becoming circular far from the core[14]. This causes only the tip of the super-spiral waves to be seen. This restriction may be overcome in other excitable media (such as those listed in the introduction), where the spiral waves exhibit highly meandering tip motion. □

Received 9 July; accepted 29 August 1991.

1. Allesie, M. A., Bonke, F. I. M. & Schopman, T. Y. G. *Circulation Res.* **33,** 54–62 (1973).
2. Goroleva, N. A. & Bures, J. *J. Neurobiol.* **14,** 353–363 (1983).
3. Robertson, A. & Grutsch, A. F. *Cell* **24,** 603–611 (1981).
4. Devreotes, P. N., Potel, M. J. & MacKay, S. A. *Devl. Biol.* **96,** 405–415 (1983).
5. Muller, S. C., Plesser, T. & Hess, B. *Physica* D**24,** 71–86 (1987).
6. Agladze, K. I., Krinsky, V. I. & Pertsov, A. M. *Nature* **308,** 834–835 (1984).
7. Zhabotinsky, A. M., Zaikin, A. N. in *Oscillatory Processes in Biological and Chemical Systems*, Vol. 2 (in Russian) (Nauka, Pushchino, 1971).
8. Zykov, V. S. *Biofizika* **31,** 862–865 (1986); **32,** 337–340 (1987).
9. Skinner, G. S. & Swinney, H. L. *Physica* D**48,** 1–16 (1991).
10. Winfree, A. T. *Science* **175,** 634–636 (1972); **181,** 937–939 (1973).
11. Perez-Muñuzuri, V. & Hanusse, P. *J. nonlinear Sci.* (in the press).
12. Perez-Muñuzuri, V., Aliev, R., Vasiev, B. & Krinsky, V. I. *Physica* D (submitted).
13. Agladze, K. I., Krinsky, V. I., Panfilov, A. V., Linde, H. & Kunhert, L. *Physica* D**39,** 38–42 (1989).
14. Meron, E. *Physica* D**49,** 98–106 (1991).
15. Hanusse, P., Perez-Muñuzuri, V. & Vidal, C. in *Nonlinear Wave Processes in Excitable Media, NATO ASI Series B: Physics Vol. 244* (eds Holden, A. V., Markus, M. & Othmer, H. G.) 501–512 (Plenum, New York, 1991).

ACKNOWLEDGEMENT. V.P.M. thanks P. Hanusse for discussions.

A 13,000-year climate record from western Tibet

F. Gasse*, M. Arnold†, J. C. Fontes*, M. Fort‡, E. Gibert*, A. Huc§, Li Bingyan‖, Li Yuanfang‖, Liu Qing*, F. Mélières¶, E. Van Campo#, Wang Fubao & Zhang Qingsong‖**

* Laboratoire d'Hydrologie et de Géochimie Isotopique, Bâtiment 504, Université Paris-Sud, 91405 Orsay Cedex, France
† Centre des Faibles Radioactivités, CEA-CNRS, BP 1, Avenue de la Terrasse, 91198 Gif-sur-Yvette Cedex, France
‡ Laboratoire de Géographie Physique, Université Paris 7, 2 Place Jussieu, 75251 Paris Cedex 05, France
§ Institut Français du Pétrole, B.P. 311, 92506 Rueil-Malmaison Cedex, France
‖ Institute of Geography, Chinese Academy of Science, Beijing 100012, China
¶ Laboratoire de Géologie, Muséum d'Histoire Naturelle, 51 rue de Buffon, 75005 Paris, France
# Laboratoire de Géologie du Quaternaire, Faculté des Sciences de Luminy, Case 907, 13288 Marseille Cedex 2, France
** Department of Geography, Nanjing University, Nanjing, China

ALTHOUGH the Tibetan plateau is important in influencing the atmospheric circulation of the Northern Hemisphere[1–3], there are only a few continuous palaeoclimate records available, and these are limited to the plateau's northeastern margin[4–6]. Here we present a 13,000-yr record from Sumxi Co (western Tibet), constructed from both lake-core and shoreline studies, which shows that conditions in the early–middle Holocene were warmer and wetter than at present. These results confirm model predictions of an intensified monsoon over the region at ~9,000 yr BP, owing to an orbitally induced increase in summer insolation[7,8]. We also find evidence for warm, humid pulses at ~12,500 and ~10,000 yr BP, in phase with the steps of the last deglaciation, and for a return to cold, dry conditions at ~11–10,000 yr BP, none of which can be explained by orbital variations. The existence of the cold episode confirms that the cooling associated with the Younger Dryas event occurred in continental China[6,9], and provides further evidence of the global nature of this event[10].

The 1989 Sino-French expedition (Kunlun-Karakorum Programme, CNRS-Academia Sinica) investigated lakes in western Tibet (mean elevation >5,000 m above sea level), the coldest and driest part of the Tibetan-Qinghai plateau[11]. Located in the rain shadow of two high mountain ranges, the Kunlun and the Karakorum (Fig. 1*a*), the region receives rare summer convective precipitation (<50 mm yr^{-1}) and on exceptional occasions, monsoon rainfall (Table 1). Ratios of evaporation to precipitation range between 20 and 50 (ref. 12). Tibetan lakes have experienced large changes in water level after the last glacial maximum (LGM)[6,12–15], in response both to warming which induced melting of previously accumulated ice, and to changes in precipitation–evaporation balances, although some lake fluctuations might have tectonic causes.

Sumxi Co (Co means lake; Fig. 1), a lake of tectonic origin[16], is very sensitive to regional climate changes because (1) it lies outside the direct influence of the highest mountains and large ice caps; (2) neotectonics[16] have not significantly modified its hydrology; (3) it is supplied by melt water from small glaciers[17] and local rainfall on a restricted catchment area (Fig. 1*b*; Table 1). The glaciers lie on granite, whereas most of the watershed

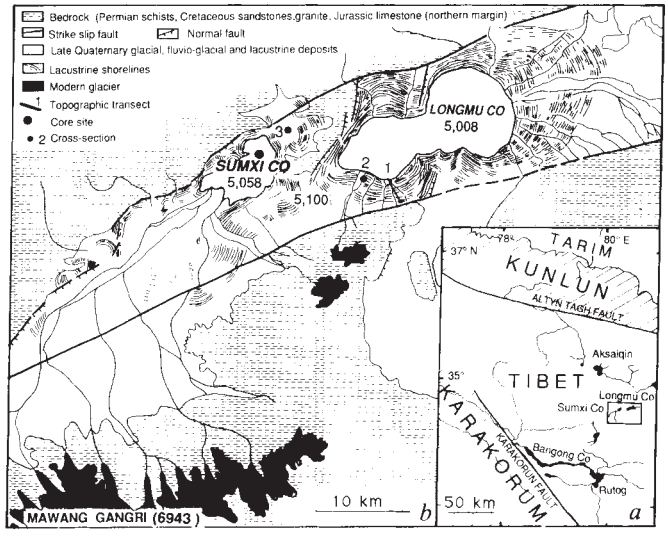

FIG. 1 *a*, Location map of Sumxi Co in western Tibet. *b*, The Lungmu Co and Sumxi Co basin.